Security X-ray Screening with Modulated-Energy Pulses

Anatoli Arodzero
RadiaBeam Technologies, LLC
Santa Monica, CA USA
arodzero@radiabeam.com

Salime Boucher
RadiaBeam Technologies, LLC
Santa Monica, CA USA

Paul Burstein
RadiaBeam Technologies, LLC
Santa Monica, CA USA

Sergey V. Kutsaev
RadiaBeam Technologies, LLC
Santa Monica, CA USA

Richard C. Lanza
Massachusetts Institute of Technology
Cambridge, MA USA

Vincent Palermo
Vertilon Corporation
Westford, MA USA

***Abstract*— This paper provides a brief overview of new screening methods that employ Modulated-Energy X-ray Pulses (MEXP) to provide a number of near-simultaneous multi-energy measurements in transmission-, backscatter-, and Computed Tomography (CT) security systems.**

In transmission X-ray cargo screening, these multi-energy measurements improve material discrimination, maximize penetration, and enhance contrast resolution while simultaneously reducing inspection time and dose to the environment, thus resulting in a smaller exclusion zone.

In backscatter systems, the use of this method will increase penetration and improve image quality of concealed objects located deeper below the surface. Specifically, different depths within an object can be probed simultaneously.

In CT, our MEXP approach mitigates the main disadvantages of the conventional dual-energy technique: a) distortion of image of the boundaries between regions with large difference in density; b) limited range of object thickness where material decomposition is valid; c) ambiguity and artifacts caused by sampling different regions due to motion of the object between interlaced pulses with distinct energies.

Results of testing of the prototype of high speed Adaptive, Multi-Energy Cargo Inspection System (AMEXIS) will be presented. Progress in the development of MEXP-based backscatter inspection system, and systems for cargo screening with Adaptive CT will also be shown.

Keywords*— *Cargo screening; Cargo Inspection; Contraband detection; X-ray radiography; X-ray backscatter; Computed Tomography.

I. Introduction: Transmission X-ray Screening Using Modulated-Energy Pulses

The concept of modulated-energy X-ray screening technique is explained below using the Adaptive Multi-Energy Inspection System (AMEXIS) as an example. The AMEXIS idea, Fig.1, relies on a linac-based, adaptive, ramped-energy source of packets of short X-ray pulses sampled by a new type of fast X-ray detector with rapid hardware processing for intelligent linac control, advanced radiography image processing, and material discrimination analysis [1-5].

A packet of X-ray pulses with increasing energy produced by linac allows adaptive multi-energy material discrimination in a single scan line. Feedback from the detection system is used for real-time adjustment of the duration of the next packet to adjust beam end-point energy to the areal density of inspected cargo.

In contrast to a previously suggested intrapulse multi-energy X-ray cargo inspection method [6], the X-ray beam consists of temporal sequence of packets of short pulses (250 – 400 ns) separated by small time intervals (50 – 150 ns). This technique addresses the SiPM's speed limitation caused by their recovery time, and results in an increased detector dynamic range [1, 7], corresponding to greater penetration depth and material discrimination range.

The higher electron beam current at low energies at the beginning of packet provides sufficient X-ray flux for material discrimination. The lower electron current partially compensates for greater bremsstrahlung flux at high energy pulses in the packet.

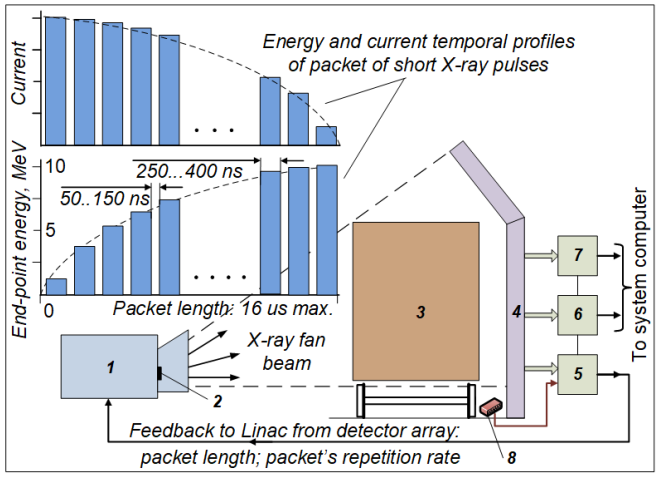

Fig. 1. AMEXIS Concept. 1 - Electron linac; 2 – X-ray converter; 3 – Cargo under interrogation; 4 – Linear array of fast detectors; 5 – Fast processor for linac control; 6 – Radiographic image processor; 7 – Material discrimination processor; 8 – Cargo speed sensor.

Intelligent material discrimination

AMEXIS detectors collect the dual energy data for material discrimination within the same scan line provided by a

ramping energy packet of short X-ray pulses by separately acquiring pulses within the packet, Figure 2. This way both high and low energy detector readings belong to the same region of cargo.

For an X-ray pulse within the ramping-up energy packet, until time t_B, Figure 2, there is no detector pixel response because the X-ray pulse does not yet contain photons of sufficient energy to penetrate the region of cargo sensed by the given pixel. Once a penetrating end-point energy is reached, the detector
pixel response starts increasing along with the increasing end-point energy of the X-ray pulse. For a given X-ray pulse and detector responsivity, the time t_B depends only on the areal density of the region of cargo and its material composition characterized by the effective atomic number Z_{eff} [1, 2].

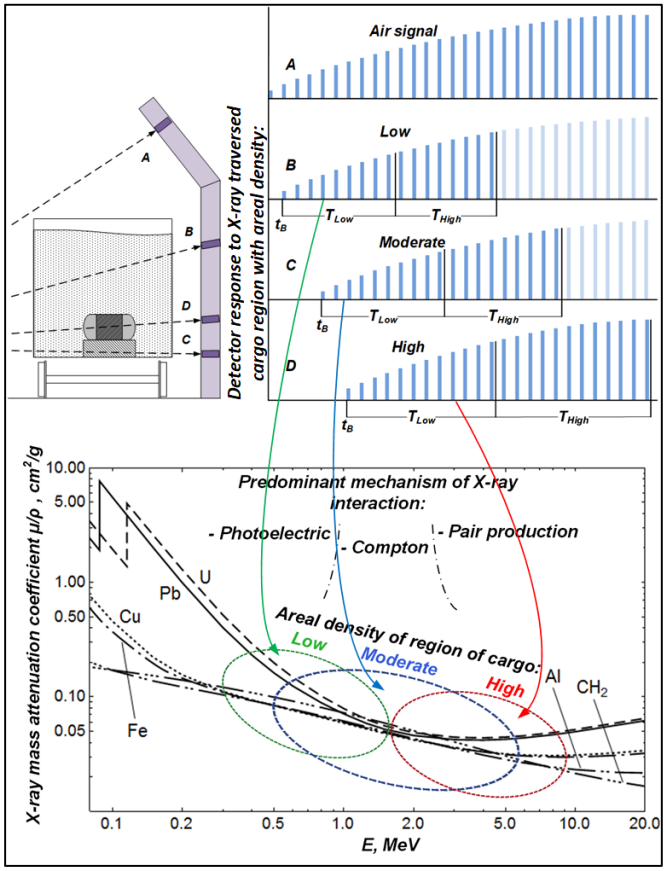

Fig. 2. Intelligent selection of the optimal X-ray energy range for dual-energy material discrimination in given region of cargo is based on measured areal density of this region, sensed by corresponding pixel of detector array.

One of the main advantages of the described technique is the ability to intelligently select the range of X-ray energy optimal for the material discrimination. The choice of higher and lower end-point energies, guided by the measured cargo attenuation, provides equally effective material discrimination for low-, high-, and particularly difficult moderate- areal densities of a region of cargo, Figure 2 bottom. Essentially, the continuous beam energy ramp provides an additional dimension for the material discrimination algorithm. Such a capability allows the possibility of exploring iterative material discrimination algorithms, previously unfeasible due to hardware limitations. These algorithms extend the region of material discrimination validity, improve overall material discrimination and will achieve additional highly desirable material discrimination capabilities (such as lead vs. uranium) in certain attenuation regions.

AMEXIS Proof-of-Concept test

The Proof-of-Concept test of AMEXIS, Figure 3, was conducted at RadiaBeam High Energy Test Facility in Santa Monica, CA.

Figure 4 shows ratio R for materials (lead, steel, aluminum, polyethylene) as a function of equivalent steel thickness. All four materials are clearly separated, demonstrating the efficacy of the AMEXIS technique for material discrimination. Eight packets of ramping energy pulses were used to generate each data point.

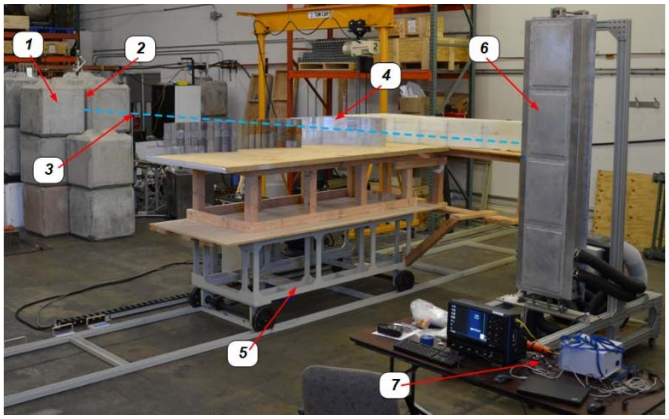

Fig. 3. Proof-of-Concept AMEXIS deployment at RadiaBeam High Energy Test Facility. *1* - Concrete shielding around 9 MeV linac; *2* - Slot with vertical steel fan collimator; *3* - Main axis of the vertical fan beam; *4* - Four materials step wedges absorber; *5* - Motorized trolley; *6* - 256-channel detector array; *7* - Data acquisition unit and power suppliers.

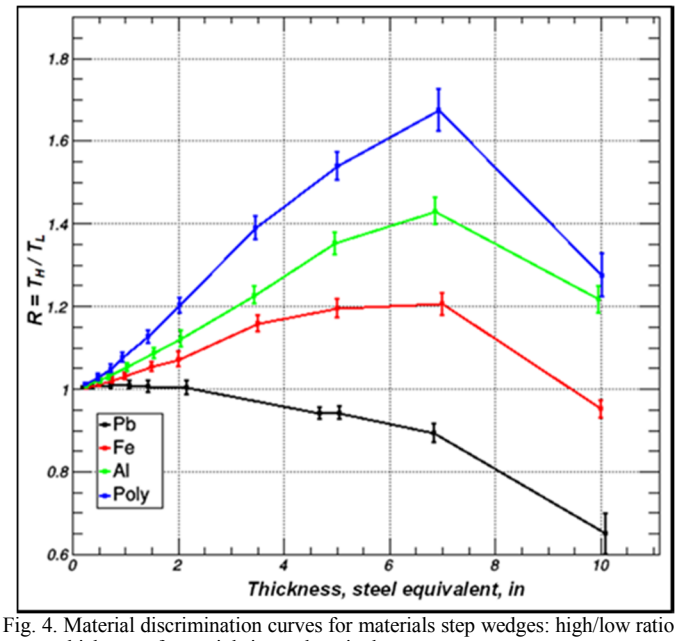

Fig. 4. Material discrimination curves for materials step wedges: high/low ratio versus thickness of materials in steel equivalent.

978-1-7281-5092-5/19/$31.00 ©2019 IEEE

Figure 5 shows gray-scale and color-coded images of step wedges generated by the material discrimination algorithm. To assign ***Z***-dependent color and color density, the algorithm uses the high/low energy ratio ***R*** (T_H/T_L), and attenuation measurements from a single scan.

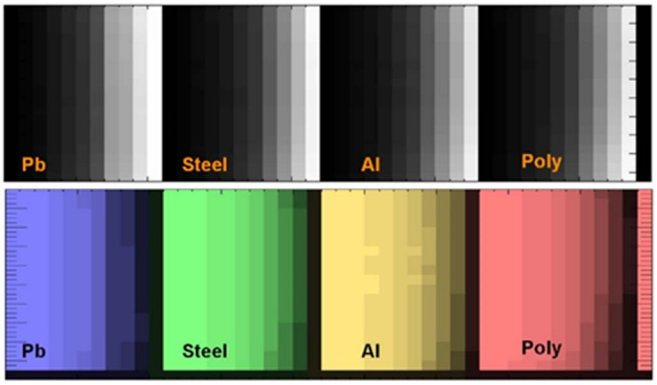

Fig. 5. Gray-scale and Color-coded images of four materials step wedges.

The design characteristics of the AMEXIS in cargo trains inspection version are presented in Table I.

TABLE I. PARAMETERS OF 9 MEV AMEXIS SYSTEM FOR CARGO TRAINS SCREENING

	Conventional dual energy interlaced system	*AMEXIS*
Maximum scanning speed with material discrimination	*15 km/h*	*45 km/h*
Sampling rate at 45 km/h	*37%*	*100%*
Material discrimination range of thickness, steel equivalent	*45-200 mm*	*6-250 mm*
Number of Z-groups of material discrimination	*3*	*4*
Penetration, steel equivalent	*330 mm*	*> 425 mm*
Contrast sensitivity at 45 km/h (at 200 mm steel)	*4%*	*1.5%*
Wire detection in air	*1.0 mm Cu*	*0.8 mm Cu*
Wire detection at speed 45 km/h	*5.0 mm Cu*	*<2.0 mm Cu*
Dose rate per scan line, moderately load cargo, cGy	*0.210*	*0.125*
Scan Tunnel size (W x H)	*3.6 x 6.2 m*	*3.6 x 6.2 m*

II. ADAPTIVE COMPUTED TOMOGRAPHY WITH MODULATED-ENERGY X-RAY PULSES

The key advantage of the Adaptive Computed Tomography with Modulated-Energy X-ray Pulses, ACTM, Figure 6, is that each elementary pencil beam (which makes up the cone beam) collects multi-energy data over many different and selectable energy bands, compared with only two energies for conventional dual-energy methods [8].

With ACTM, the scan rate can be doubled, and accurate multi-energy band data can be processed into material distribution maps. ACTM also mitigates the main disadvantages of conventional dual-energy methods: a) ambiguity and artifacts caused by sampling different regions due to motion of the object between interlaced pulses with distinct energies; b) distortion of the reconstructed image's boundaries between regions with large differences in density; c) small range of object thickness where material decomposition is valid. Filtered Backprojection (FBP) can be used in a helical image reconstruction. We employ the theoretically exact and fast *Katsevich algorithm* [9-11] with a three-step procedure for CT imaging reconstruction.

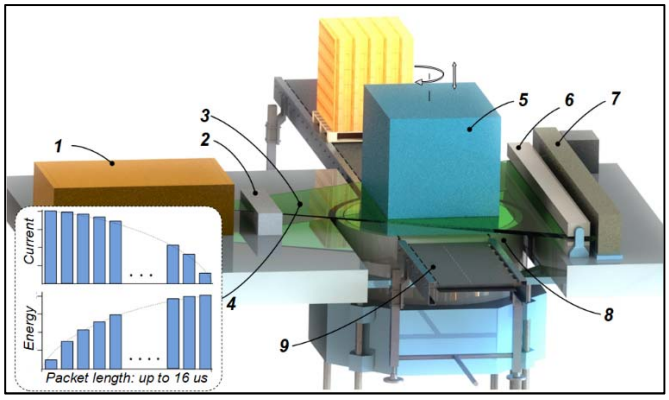

Fig. 6. Schematic layout of ACTM system for air cargo and small containers screening. ***1*** - Linac; ***2*** - Precollimator; ***3*** – Collimated X-ray cone beam; ***4*** – Temporal profile of one packet in the X-ray cone beam; ***5*** – Air cargo container; ***6*** – Collimator; *7* – 2D array of fast, time resolving detectors; ***8*** – Rotating elevator; ***9*** – Conveyor belt.

An experimental setup for tuning ASTM technique is shown in Figure 7.

Fig. 7. 256-channel detector array and rotary table for the inspected objects in preparation for the CT measurements with 6 MeV linac. ***1*** – Main axis of X-ray cone beam; ***2*** – Motorized rotary table with remote control; ***3*** - Detector array (the covers are open).

Few-View CT Approach

The combination of cone-beam of Modulated-Energy X-ray Pulses and 2D array of transmission detectors can be used to produce few-view tomographic images of cargo in motion. In the special cases of inspecting cargo of known constructions and relatively simple content, e.g., grain or liquids, or regular geometries, the search for anomalies becomes much simpler than screening of a cargo of completely unknown contents. In the first case, there is little entropy in any of the views, and the background of known cargo geometry can be subtracted. Anything remaining is ideally uniform, and anomalies will be readily apparent in any view. The same is true of periodic, known structures, e.g., prepackaged groups of known, regular small objects, where an absorption template of expected pattern can be subtracted from the 3D data; any anomaly will be flagged. In both of these cases, far fewer views than required in conventional CT are necessary to detect, locate, and identify

978-1-7281-5092-5/19/$31.00 ©2019 IEEE

any anomalies. Therefore, Algebraic Reconstruction Techniques and derivative approaches [12, 13] are appropriate. Very few-view imaging can also employ stationary sets of x-ray source/detector array pairs and require no rotary motion.

III. Backscatter Deep Imager for Robotic or Handheld Operations

Conventional backscatter inspection systems, whether fixed or mobile, use X-ray tubes that generate an unmodulated bremsstrahlung beam with end-point energy in the range of 100 to 240 keV. Such systems allow good visualization of low-*Z* objects directly behind the metal wall with a thickness of 1.5 - 4.0 mm (car body, cargo containers, aircraft components). Low-*Z* materials show up in the scatter images as bright areas that have relatively high photon counts.

Performance of conventional backscatter systems (penetration depths, spatial resolution, and contrast of concealed objects) is limited by the backscatter signal from the front surface of the inspected item.

To overcome this fundamental limitation, we employ a pencil X-ray beam with a train of modulated energy/current pulses, fast, time-resolving X-ray detectors, and an algorithm of image "peeling" processing [14]. Sequencing energy and current of the X-ray beam allows separation of backscatter signals originating from the various depths of inspected item. This approach provides deeper penetration, greater material discrimination, improved spatial resolution, and enhanced contrast of objects within the concealed volume.

Schematic layout of 120 keV backscatter deep scan imager (DeepBx), version for robotic or handheld operation, is shown in Figure 8.

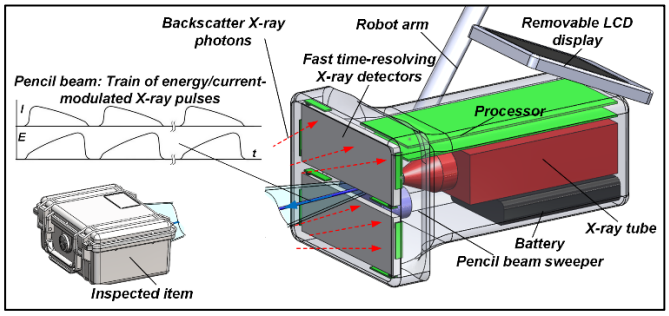

Fig. 8. 120 keV DeepBx imager for handheld or robotic operation.

Figure 9 shows another version of DeepBx: Tracked rover with mounted linac-based backscatter deep imager. This remote-controlled security screening system uses an ultra-compact 1 MeV Ku-band linac [15].

The backscatter technique using the MEXP approach will allow visualization of objects at a depth inaccessible to existing methods.

IV. Sources of Energy-Modulated X-ray Pulses

Energy-modulated X-ray pulses are generated with either X-ray tubes or linacs, depending on the required pulse energy. Below 240 keV, X-ray tubes are the optimal choice for security inspection systems: they are compact, robust and can provide high currents. X-ray energy modulation is achieved by applying a voltage ramp to the accelerating gap.

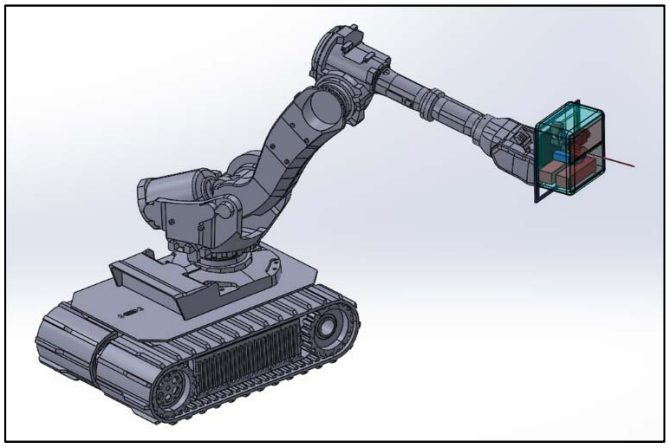

Fig. 9. Tracked rover with mounted 1 MeV linac-based backscatter deep imager.

In order to enable novel adaptive screening systems for both radiography and CT, new types of X-ray sources are being developed at RadiaBeam [15-17]. Depending on the application, the range of the beam energies can vary from 1 to 9 MeV, Table II.

Table II. Core Parameters of X-ray Sources for Adaptive Screening Systems

System	Energy, MeV	Linac	RF source
Portal; R/r	6; 9	S-band	Klystron
Mobile	4; 6	X-band	Magnetron
Compact	1	Ku-band	Magnetron

For portal and rail cargo screening systems, high beam power and energy range are the core drivers for the accelerator design, so a traveling wave S-band (10 cm wavelength) klystron-driven linac is a reasonable choice. For such applications, RadiaBeam has developed a linac with envelope energy of packet of X-ray pulses ramps from 2 to 9 MeV, as shown in Figure 10. Figure 11 shows examples of temporal profiles of X-ray pulses that can be generated by this linac.

Currently there is strong interest in accelerator systems that are compact and light enough to be placed in a lightweight truck chassis (one that does not require a commercial driver's license). For such a system, the end-point energy range can be lower, i.e. 4-6 MeV. In our linac design, Figure 12, we were able to reduce the size of all linac components by utilizing an X-band frequency accelerator carefully optimized to minimize size, and by careful design of the rest of the system. X-band standing-wave cavities have a short filling time, comparable to that of S-band travelling wave linacs described above, which is critical for the adaptive-energy regime.

For backscatter screening DeepBx imager we develop a subcompact Ku-band linac, Figure 13. Energy modulation is achieved by controlling the RF power and gun current, and utilizing the beam loading effect [1, 15].

978-1-7281-5092-5/19/$31.00 ©2019 IEEE

V. Detectors for MEXP Screening Systems

To study AMEXIS and adaptive CT inspection methods, a unified 32-channel detector module was developed, Figure 14, which also allows the use of various detector materials.

Fig. 10. Traveling wave S-band MEXP linac for radiography and CT screening.

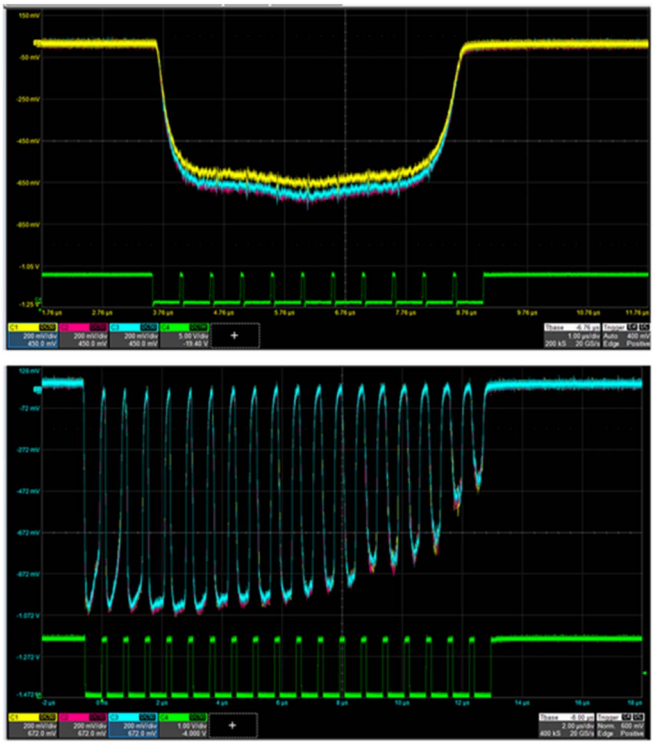

Fig. 11. Examples of temporal profiles of X-ray pulses generated by traveling wave S-band linac. Top: 9 MeV 5-microsecond X-ray pulse. Bottom: 14-microsecond ramped-energy (from 2 to 9 MeV) packet of 19 X-ray pulses. The response of the 3 adjacent detector channels, $PbWO_4$ pixels with SiPM readout, to the X-ray passed through air is shown. The green trace at the bottom of the oscillograms shows the DAQ synchronization pulses. In both cases the detector array is placed at a distance of 10 m from the X-ray converter.

Thirty-two detector channels are assembled on a modular circuit board assembly referred to as a Detector Module Board (DMB). Each detector channel on a DMB is processed through its own dedicated signal processing chain that includes SiPM bias, preamplification, signal integration, and digitization. Additionally, each channel employs its own high-speed responsivity control circuitry to dynamically adjust the SiPM operation point based on real-time measurements of the input signal [1, 2]. Up to eight DMBs are serially connected to create a PoC system of up to 256 channels, Figure 3. The DMB circuit board chain connects through a single cable to the Data Acquisition Unit (DAU), which, through a computer interface, is responsible for system configuration, data collection, and real-time diagnostics.

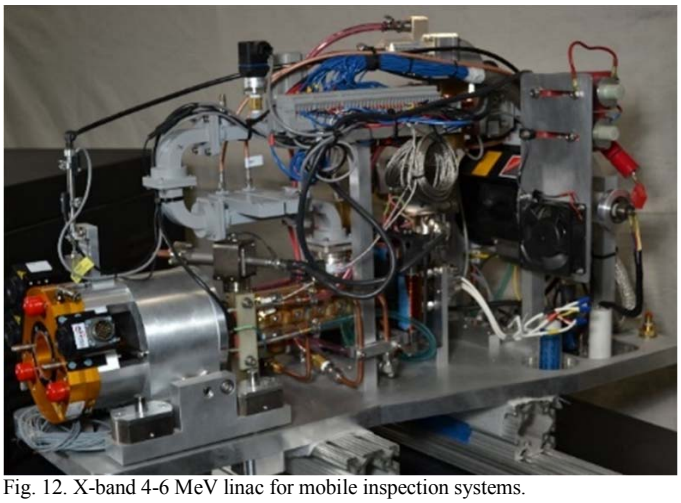

Fig. 12. X-band 4-6 MeV linac for mobile inspection systems.

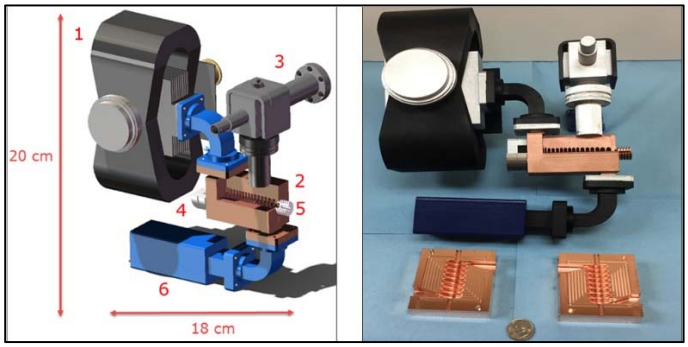

Fig. 13. Left: 3D model of the Ku-band linac head including **1**- magnetron, **2** – split accelerating structure, **3** – vacuum pump, **4** – electron gun, **5** – X-ray converter, **6** – RF load. Right: 1:1 scale 3D printed model with fabricated copper prototype halves.

For CT systems using a conical X-ray beam, a 32-channel 2D detector sub-module is being developed, Figure 15, which will employs a 256x8 detector matrix.

Detectors in AMEXIS and in adaptive CT systems are Scintillation-Cherenkov detectors [1, 2]. The material in these detectors is lead tungstate ($PbWO_4$), or fluorophosphate glass, slightly doped with Cerium [18]. For DeepBx imagers, we are developing detectors based on YSO:Ce [19], and on fluorophosphate glass highly doped with Cerium.

978-1-7281-5092-5/19/$31.00 ©2019 IEEE

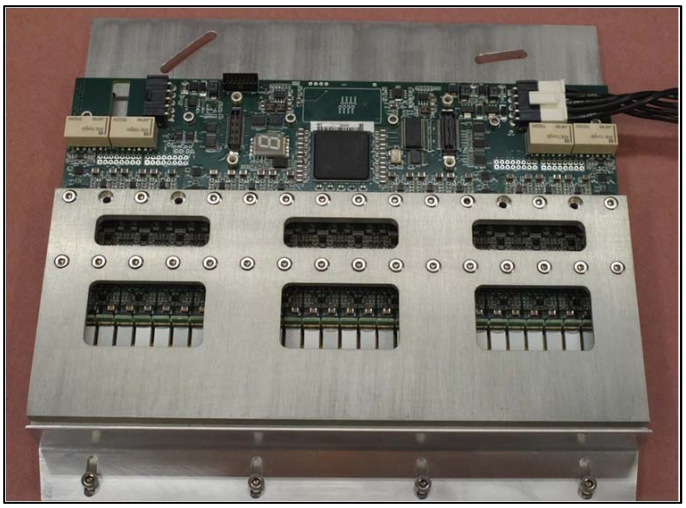

Fig. 14. 32-channel high energy X-ray detector module for AMEXIS and CT.

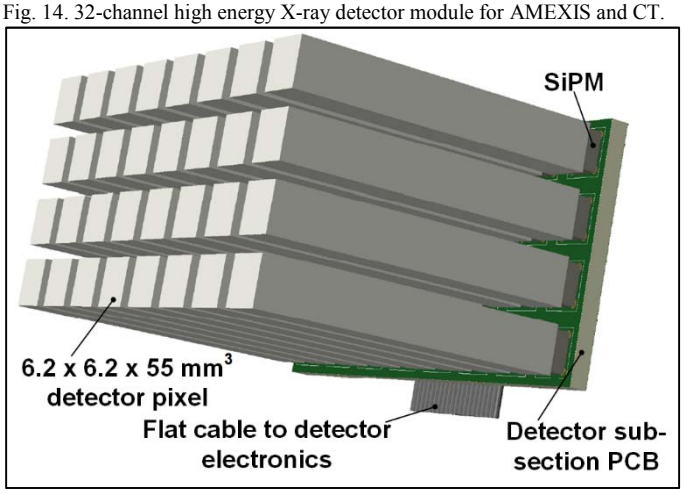

Fig. 15. 32-channel sub-module for adaptive CT systems with cone X-ray beam.

CONCLUSION

We have introduced a novel technique for transmission, CT and backscatter X-ray security screening system. This technique is based on Modulated-Energy X-ray sources, fast detectors capable of resolving the temporal intensity profile of an X-ray pulse, and intelligent detector signal processing algorithm. The underlying MEXT technology approach offers significant improvement over any currently available X-ray screening methods. Our Proof-of-Concept tests have already demonstrated the feasibility of this approach; the next phase of testing will verify predicted performance of the MEXT approach.

ACKNOWLEDGMENT

This work has been partly supported by the US Department of Homeland Security, Domestic Nuclear Detection Office, under competitively awarded contracts HSHQDC-13-C-B0019, HSHQDC-15-C-00032, HSHQDC-15-C-B0022, HSHQDC-15-C-B0025 and by the US Department of Energy, Office of Defense Nuclear Nonproliferation, under SBIR award DE-SC0015722. This support does not constitute an express or implied endorsement on the part of the Government.

REFERENCES

[1] A. Arodzero, S. Boucher, A. Murokh, S. Vinogradov, S. Kutsaev. System and Method for Adaptive X-ray Cargo Inspection. US Patent Application 2015/0338545.

[2] A. Arodzero, S. Boucher, J. Hartzell, S. Kutsaev, R. C. Lanza, V. Palermo, S. Vinogradov, V. Ziskin. High Speed, Low Dose, Intelligent X-ray Cargo Inspection. Talk N2B1-6 at IEEE-2015 Nuclear Science Symposium. DOI: 10.1109/NSSMIC.2015.7581836.

[3] A. Arodzero, S. Boucher, S.V. Kutsaev, V. Ziskin. MIXI: Mobile Intelligent X-Ray Inspection System. IEEE Transactions on Nuclear Science, 64, 7, (2017) 1629-1634.

[4] S.V. Kutsaev, R. Agustsson, A. Arodzero, S. Boucher, J. Hartzell, A. Murokh, F. O'Shea, A.Yu. Smirnov. Electron Accelerators for Novel Cargo Inspection Methods. Physics Procedia, 90 (2017) 115-125.

[5] A. Arodzero, S. Baucher, S.V. Kutsaev, R.C. Lanza, V. Palermo, A.Yu. Smirnov, S. Vinogradov. Transmission Cargo Inspection with Ramping-Energy X-ray Pulses. Invited talk #146 at Conference on the Application of Accelerators in Research and Industry CAARI-2018, Grapevine, TX, USA, August 12-17, 2018.

[6] A. Arodzero, M. Rommel, A. Saverskiy, R. Sud. System and methods for intrapulse multi-energy and adaptive multi-energy X-ray cargo inspection, U.S. Patent 8,457274.

[7] S. Vinogradov, A. Arodzero, R.C. Lanza. Performance of X-ray detectors with SiPM readout in cargo accelerator-based inspection systems. Presented at IEEE-2013 NSS. DOI:10.1109/NSSMIC.2013.6829597.

[8] A. Arodzero, P. Burstein, R. Lanza. Adaptive Computed Tomography with modulated-energy X-ray pulses. US Provisional Patent Application.

[9] A. Katsevich. Improved exact filtered back-projection algorithm for spiral CT. Advances in Applied Mathematics, 32, (2004), 681-697.

[10] A. Katsevich. Method of reconstructing images for spiral and non-spiral computer tomography, US Patent 6,771,733, 2004.

[11] F. Giudiceandrea, A. Katsevich, and E. Ursela. A Reconstruction Algorithm is a Key Enabling Technology for a New Ultrafast CT Scanner. SIAM News, November 2016.

[12] L. Flores, V. Vidal, G. Verdu. Iterative Reconstruction from Few-View Projection. Procedia Computer Science, 51, 2015 703-712.

[13] A.Yazdanpanah, E. Regentova, G. Bebis. Algebraic Iterative Reconstruction-Reprojection Method for High Performance Sparse-View CT Reconstruction. Appl. Math. Inf. Sci 10, 6, 1-8 (2016).

[14] A. Arodzero, S. Kutsaev, V. Ziskin. X-Ray Backscatter Inspection System. US Patent Application 2017/0336526.

[15] S.V. Kutsaev, R. Agustsson, A. Arodzero, S. Boucher, A. Murokh, A.Yu. Smirnov. Sub-MeV ultra-compact linac for radioactive isotope sources replacement, non-destractive testing, security and medical applications. NIM B, (2019) https://doi.org/10.1016/j.nimb.2019.08.029.

[16] S.V. Kutsaev, R. Agustsson, A. Arodzero, S. Boucher, J. Hartzell, A. Murokh, F. O'Shea, A.Yu. Smirnov. Electron Accelerators for Novel Cargo Inspection Methods. Physics Procedia, 90 (2017) 115-125.

[17] S.V. Kutsaev, R. Agustsson, A. Arodzero, S. Boucher, P. Burstein, A. Yu. Smirnov. X-ray Sources for Adaptive Radiography and Computed Tomography. Physics Procedia, 2018 (in press).

[18] C. Hu, Al. Margaryan, As. Margaryan, F. Yang, L. Zhang, R-Y. Zhu. Alkali-free Ce-doped and co-doped flurophosphate glasses for future HEP experiments. NIM A (2018), doi.org/10.1016/j.nima.2018.11.124.

[19] M. Moszynski, M. Balcerzyk, M. Kapusta, D. Wolski, C. Melcher. Large size LSO:Ce scintillators and YSO:Ce for 50 MeV range gamma-ray detector. IEEE -1999 NSS, DOI: 10.1109/NSSMIC.1999.845759.